Improvement to the PML Boundary Condition in the FEM Using Mesh Compression

Arnan Mitchell, *Member, IEEE*, David M. Kokotoff, *Member, IEEE*, and Michael W. Austin, *Member, IEEE*

***Abstract*—Numerical errors encountered when using the perfectly matched layer (PML) absorbing boundary condition with the finite-element method are investigated to discover more efficient implementation schemes. Closed-form expressions for the numerical reflection at an interface between two general biaxial materials are applied to the special case of a PML boundary. Expressions for an anisotropically compressed mesh are then derived, revealing that reflections can be greatly reduced through increasing mesh density only where it is required. Significant improvements over previously reported PML boundaries are demonstrated.**

***Index Terms*—Finite-element methods, numerical errors, PML.**

I. Introduction

THE finite-element method (FEM) has become an invaluable tool for the analysis of electromagnetic problems with complex geometries. In particular, the three-dimensional (3-D) FEM allows for the rigorous analysis of a broad range of practical structures. The routine use of the FEM in design problems can, however, become cumbersome due to the vast computational resources often required.

It is interesting to note that a significant proportion of the unknowns in typical problems are utilized in modeling the free space separating the geometry of interest from the boundary condition that terminates the solution space. Small reflections from these terminating boundaries, due to their imperfect implementation, can significantly affect the finite-element solution. Increasing the distance from the geometry of interest to the terminating boundary can minimize the effects of these reflections.

The increase in distance to the terminating boundary comes at the cost of an increased number of elements, an effect that can become crippling when considering 3-D models. Thus, much attention has been paid to the reduction of reflection errors from these boundaries. The reflectionless perfectly matched layer (PML) boundary [1], [2] offers great promise for the reduction of these reflections, however, as discussed in [3], the PML boundary condition, when applied to the FEM, is not, in fact, reflectionless. It would seem that in order to implement a PML boundary that sufficiently reduces these reflections, an excessive number of unknowns is required, defeating the purpose of including such a boundary.

Manuscript received May 3, 2000.

A. Mitchell and M. W. Austin are with the Department of Communication and Electronic Engineering, Royal Melbourne Institute of Technology University, Melbourne, Vic. 3000, Australia.

D. M. Kokotoff was with the Royal Melbourne Institute of Technology University, Melbourne, Vic. 3000, Australia. He is now with Gabriel Electronics, Scarborough, ME 04074 USA.

Publisher Item Identifier S 0018-9480(02)04066-8.

An investigation [4] has developed expressions for the reflection coefficient from a PML interface in a finite-difference time-domain (FDTD) model on a rectangular grid for interfaces between isotropic media and a PML truncation. We have previously investigated the nature of reflection errors caused by triangular finite-element discretization at boundaries in biaxial materials [5], deriving closed-form expressions that have proven to be a very good model of the numerical errors observed in practical finite-element simulations. A PML interface is a special case of such a boundary and, thus, those closed-form expressions should be equally well suited to the analysis of the associated numerical errors.

Section II of this investigation applies the closed-form expressions derived in [5] to the special case of a PML boundary interface. The resulting expressions are compared to practical simulations to ensure their validity and then their form is examined to better understand the behavior of the PML and how the associated numerical errors depend on the parameters of the problem. It is found that the numerical reflection error depends only on discretization parameters normal to the PML interface, suggesting that uniform mesh refinement may be an inefficient approach to suppressing numerical reflections. Thus, Section III re-derives the expressions for an anisotropically distorted mesh and the resulting expressions are again applied to the special case of the PML. A significant reduction in numerical reflections from PML boundaries is predicted and finite-element simulations verify that such gains are also obtained in practice. Comparison with the previous investigation of Polycarpou *et al.* [3] verify that an anisotropic mesh compression can offer a very efficient means of implementing a PML boundary.

II. Numerical Reflection From a PML

In [5], expressions for the numerical dispersion and reflection expected from an interface between two general biaxial materials were derived. This was done for two-dimensional triangular elements for both edge and node-basis functions. Although uniform equilateral triangles were assumed, these expressions were demonstrated to provide a reasonable approximation to a practical mesh.

It was concluded that these expressions for numerical inaccuracies could provide a useful tool for the investigation of PML performance in the FEM. An investigation of numerical dispersion and reflection of the special case of a PML boundary is thus conducted in Section II-A.

A. Closed-Form Reflection From the PML

For brevity, the closed-form expressions for numerical dispersion and reflection from an arbitrary interface between two

biaxial materials are not repeated here. It is thus recommended that the reader refer to the derivations and resulting expressions contained in [5].

The important result from this previous investigation is that material constants and mesh density of an FEM simulation can be encapsulated in the parameters

$$c_x = k_0\sqrt{\epsilon_z\mu_x}L \quad c_y = k_0\sqrt{\epsilon_z\mu_y}L. \tag{1}$$

For a TE to z polarized plane wave, and

$$c_x = k_0\sqrt{\mu_z\epsilon_x}L \quad c_y = k_0\sqrt{\mu_z\epsilon_y}L \tag{2}$$

for a TM to z polarized plane wave, where ϵ_x, ϵ_y, and ϵ_z are the components of the anisotropic permittivity, μ_x, μ_y, and μ_z are the components of the anisotropic permeability, k_0 is the free-space wavenumber, and L is the approximate edge length of the triangles in the mesh, assuming uniform equilateral triangles. It was shown in [5] that the numerical reflection error for both nodes and edges rose as the square of the parameters c_x and c_y.

Using the expressions derived in [5] to examine the reflection errors present at a PML boundary, is a simple matter of setting the material tensors to those of the PML boundary and the material that it is matching. From [6], a PML material (Material 2) that matches an arbitrary biaxial material (Material 1) at a boundary that is normal to the x-direction, must have material tensors of the form

$$\bar{\bar{\epsilon}}_2 = \begin{bmatrix} \dfrac{\epsilon_{x1}}{a_{\rm pml}} & 0 & 0 \\ 0 & a_{\rm pml}\cdot\epsilon_{y1} & 0 \\ 0 & 0 & a_{\rm pml}\cdot\epsilon_{z1} \end{bmatrix} \tag{3}$$

$$\bar{\bar{\mu}}_2 = \begin{bmatrix} \dfrac{\mu_{x1}}{a_{\rm pml}} & 0 & 0 \\ 0 & a_{\rm pml}\cdot\mu_{y1} & 0 \\ 0 & 0 & a_{\rm pml}\cdot\mu_{z1} \end{bmatrix}. \tag{4}$$

Thus, for the specific case of a PML interface, the c_x and c_y parameters of Material 2 will be

$$c_{x2} = c_{x1} \quad c_{y2} = a_{\rm pml}c_{y1}. \tag{5}$$

Thus, since c_{y2} scales with $a_{\rm pml}$, and the numerical reflection error from an arbitrary biaxial interface scales with c_y^2, the numerical reflection error from a PML interface should increase as $a_{\rm pml}^2$.

B. Verification of the Reflection Error From the PML

The numerical reflection error from a PML truncation as a function of $a_{\rm pml}$ and mesh density has been investigated in [3]. It will be instructive to reexamine this investigation and compare it to the numerical reflection predicted using the closed-form expressions of the previous section along with the c_x and c_y parameters stated above.

Following [3], the PML variable parameter is defined as

$$a_{\rm pml} = 1 - j\,\frac{3\delta}{2k_0 d} \tag{6}$$

where d is the depth of the PML layer and

$$\delta = -\ln(R) \tag{7}$$

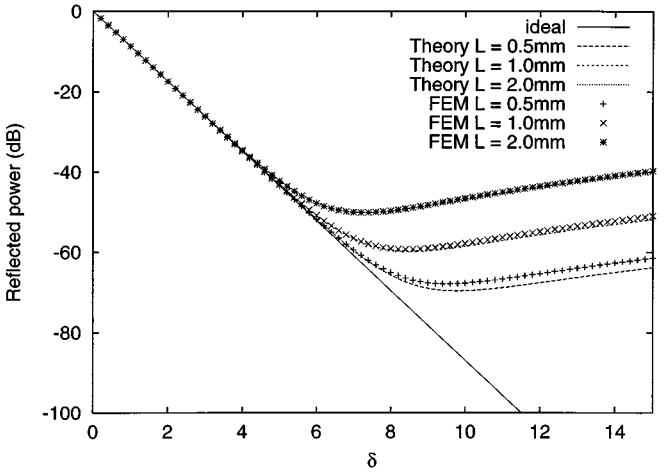

Fig. 1. Numerical reflection from a PML interface as a function of $\delta = \ln(1/R)$ for edge lengths of 2.0, 1.0, and 0.5 mm using an incident TEM mode at 100 MHz and edge-basis functions. The lines indicate the reflection predicted by the closed-form expressions, while the points represent the reflection actually observed from a finite-element simulation using a practical mesh. The ideal reflection is also shown.

in which R is the desired reflection from the PML termination.

The geometry modeled consisted of an air-filled parallel-plate waveguide, terminated with a uniform PML region backed with a perfect electric conductor. The depth of the PML is $d = 2$ cm. The software Triangle [7] was used to produce meshes for this geometry with average edge lengths of 2.0, 1.0, and 0.5 mm, respectively. The power reflected back into the input port from the PML termination was then recorded as a function of the parameter δ $(=\ln(1/R))$ for each of these mesh dimensions. The numerical reflection as predicted by the closed-form expressions of the previous sections using these mesh densities, and PML parameters were also calculated and compared to the observed reflection errors from the FEM simulation.

Fig. 1 presents the response from the geometry modeled with edge elements and excited with a TEM mode at 100 MHz. The lines show the predicted reflection for the three edge lengths comprising an initial reflection from the PML, as predicted using the closed-form expressions of [5], with parameters as given in (5). A further line represents the ideal reflection R. The points depict the reflection observed from the FEM simulation of the same structure. Excellent agreement is evident.

To demonstrate the validity of the expressions for nodes and for higher order excitations, Fig. 2 shows the same reflection response modeled with nodes and excited with the $\rm TM_1$ mode at 8 GHz. To predict the reflection from this interface with the closed-form expressions, the $\rm TM_1$ wave was decomposed into the superposition of two plane waves propagating at the angle

$$\sin(\theta) = \left(\frac{m\pi}{W}\right)\frac{1}{k_0\sqrt{\epsilon_z\mu_x}}. \tag{8}$$

It is also worth noting that the PML layer only absorbs the component of the wave traveling normal to the interface and, thus, is less effective in absorbing waves incident at an angle. This explains the more gradual slope of the ideal reflection with increasing delta when compared to Fig. 1. Excellent agreement is again evident.

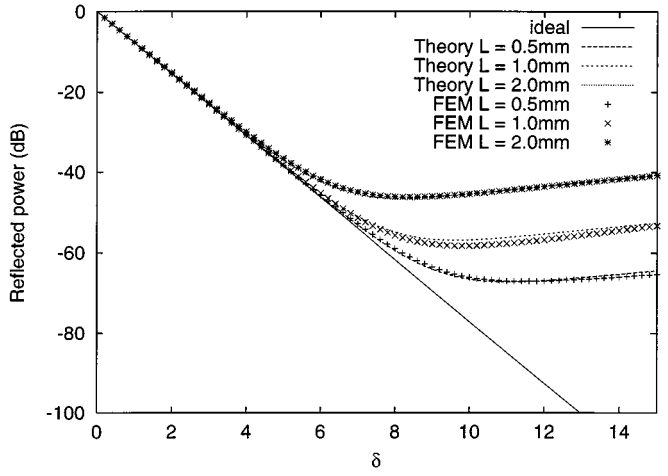

Fig. 2. Numerical reflection from a PML interface as a function of $\delta = \ln(1/R)$ for edge lengths of 2.0, 1.0, and 0.5 mm using an incident TM_1 mode at 8 GHz and node-basis functions. The lines indicate the reflection predicted by the closed-form expressions, while the points represent the reflection actually observed from a finite-element simulation using a practical mesh. The ideal reflection is also shown.

Thus, it seems that it is possible to quite accurately predict the numerical reflection from a given PML interface using the closed-form expressions of [5], as specialized in the previous section.

III. Anisotropic Discretization

Having established that the closed-form expressions of [5] provide a good model of the actual observed reflection error from a PML boundary, they can now be used to discover the nature of these numerical reflection errors and hopefully uncover a numerically efficient means of reducing these undesirable reflections.

Reduction of reflection error through reduction of L has been found to be too expensive [3]. For this reason, we now reexamine the closed-form approximations in search of a more efficient implementation.

Referring to (5), it is evident that c_{x2} is independent of the PML variable parameter a_{pml}, but that c_{y2} scales linearly with that parameter. Since the numerical reflection error varies as the square of these c-parameters, the dependence of reflection error on the PML variable parameter can be isolated to c_y only.

The approach taken by [3] in improving the effectiveness of the PML through a reduction in mesh edge length L reduces both c_x and c_y by equal amounts. It seems likely that the contribution of this edge length reduction on c_x is largely wasted and may even be counterproductive sustaining the strong anisotropy in c_x and c_y caused by a large a_{pml}. To make the most efficient use of edge length reduction in reducing the c values, it would be ideal to reduce only the contribution to c_{y2}. It is proposed that if two lengths were used to parameterize the dimensions of the triangular mesh, it may be possible to isolate these two parameters into each of the two c-parameters and, thus, it may be possible to vary only one of these parameters to most efficiently reduce the contribution of a_{pml} to the reflection error.

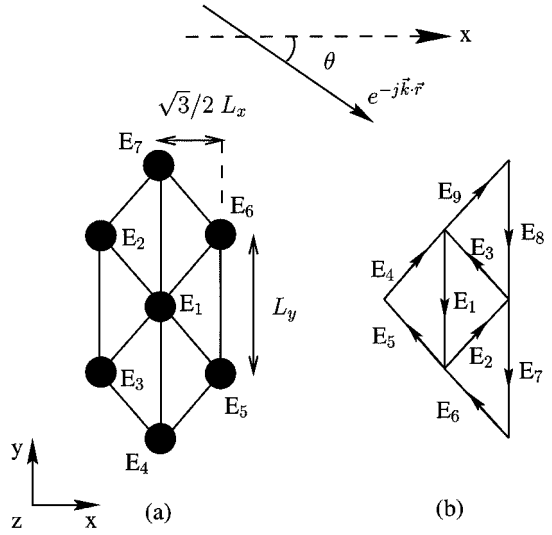

Fig. 3. Portion of an anisotropically compressed hexagonal finite-element mesh with: (a) node-basis functions and (b) edge-basis functions. The orthogonal triangle dimensions L_y and $\sqrt{3}/2\,L_x$ are labeled.

A. Derivation for Node-Basis Functions

Consider the portion of mesh depicted in Fig. 3(a). Note that the triangles comprising the mesh are now isosceles rather than equilateral, as in the derivations of [5], and are thus parameterized by two lengths L_x and L_y rather than simply L.

Directly following the procedure detailed in [5], the numerical reflection from an interface between two biaxial materials can be approximated by first calculating the numerical dispersion β_i on either side of the interface. For nodes, this is done through the solution of

$$(A_i + 2C_i) + D_i\cos(2b_i) + 2B_i\cos(a_i)\cos(b_i) = 0 \quad (9)$$

where i denotes either Material 1 or 2

$$a_i = \sqrt{3}/2c_{yi}\beta_i\cos(\theta_i) \quad b_i = 1/2c_{xi}\beta_i\sin(\theta_i) \quad (10)$$

in which θ_i is the propagation direction, relative to the x axis, of the plane wave in each material, β_i is the numerical dispersion, which should ideally be one, and

$$\begin{aligned} A_i &= 1 - 8/c_{yi}^2 \\ B_i &= 1 + 8/c_{yi}^2 \\ C_i &= 1 - 6/c_{xi}^2 - 2/c_{yi}^2 \\ D_i &= 1 + 12/c_{xi}^2 - 4/c_{yi}^2. \end{aligned} \quad (11)$$

For a TE to z polarized plane wave

$$c_{xi} = k_0\sqrt{\epsilon_{zi}\mu_{xi}}L_{yi} \quad c_{yi} = k_0\sqrt{\epsilon_{zi}\mu_{yi}}L_{xi} \quad (12)$$

while for a TM to z polarized plane wave

$$c_{xi} = k_0\sqrt{\mu_{zi}\epsilon_{xi}}L_{yi} \quad c_{yi} = k_0\sqrt{\mu_{zi}\epsilon_{yi}}L_{xi} \quad (13)$$

and L_{xi} and L_{yi} are the dimensions of the isosceles triangles for Material i, as shown in Fig. 3.

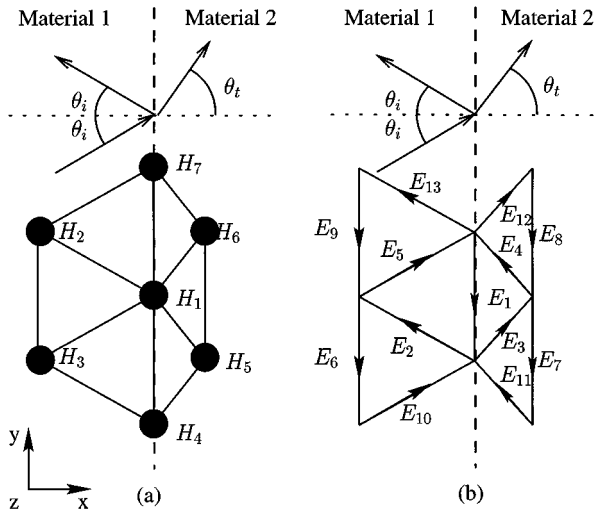

Fig. 4. Interfaces between two meshes of differing anisotropic compression for: (a) node-basis functions and (b) edge-basis functions.

A wave propagating through Material 1 and incident on a boundary to Material 2, as depicted in Fig. 4(a), will exhibit a reflection coefficient as follows:

$$r = -\frac{L_{x1}\epsilon_{z1}B_1 \sin a_1 - L_{x2}\epsilon_{z2}B_2 \sin a_2}{L_{x1}\epsilon_{z1}B_1 \sin a_1 + L_{x2}\epsilon_{z2}B_2 \sin a_2}. \tag{14}$$

Note that since the two meshes must share edges at their interface, $L_{y2} = L_{y1}$.

B. Derivation for Edge Basis

The procedure is similar for edge-basis functions with the numerical dispersion on either side being found from

$$\begin{aligned} &D_i'\left(A_i'D_i' - B_i'^2\right)\cos^2(b_i) \\ &\quad = C(A_i'C_i' - B_i'^2) - (C_i' - D_i')B_i'^2\cos(a_i)\cos(b_i) \end{aligned} \tag{15}$$

where

$$\begin{aligned} A_i' &= -c_{xi}^2 - 9c_{yi}^2 + 96 \\ B_i' &= -c_{xi}^2 + 3c_{yi}^2 + 96 \\ C_i' &= -7c_{xi}^2 - 3c_{yi}^2 + 96 \\ D_i' &= 5c_{xi}^2 - 3c_{yi}^2 + 96 \end{aligned} \tag{16}$$

from which the numerical reflection can be found as

$$r = -\frac{Z_1 - Z_2}{Z_1 + Z_2} \tag{17}$$

where

$$Z_i = \frac{(D_i'^2\cos^2 b - 4C_i'^2)}{B_i'^2(D_i' - 2C_i')\sin a_i} \tag{18}$$

in which

$$A_i' = \frac{L_{yi}}{L_{xi}}\left(-c_{xi}^2 - 9c_{yi}^2 + 96\right) \tag{19}$$

$$B_i' = \sqrt{\left(\frac{L_{yi}^2}{4L_{xi}^2} + \frac{3}{4}\right)}\left(-c_{xi}^2 + 3c_{yi}^2 + 96\right) \tag{20}$$

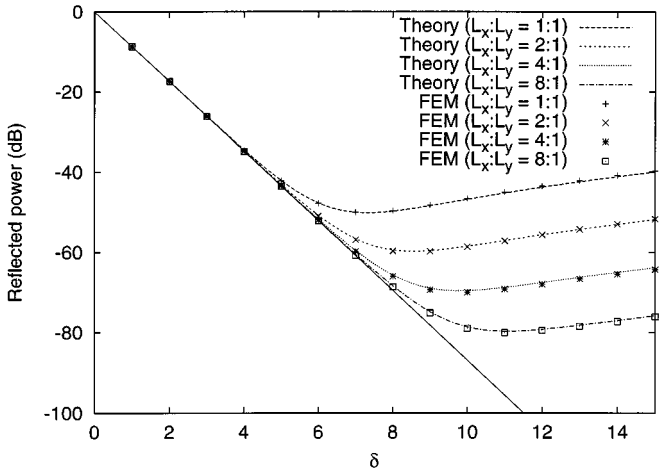

Fig. 5. Numerical reflection from a PML interface as a function of $\delta = \ln(1/R)$ with edge lengths of 2.0 mm and 1-D normal compression ratios of one, two, four, and eight in the PML region using an incident TEM mode at 100 MHz and edge-basis functions. The lines indicate the reflection predicted by the closed-form expressions, while the points represent the reflection actually observed from a finite-element simulation using a practical mesh. The ideal reflection is also shown.

$$C_i' = \frac{L_{yi}}{L_{xi}}\left(\frac{L_{yi}^2}{4L_{xi}^2} + \frac{3}{4}\right)\left(-7c_{xi}^2 - 3c_{yi}^2 + 96\right) \tag{21}$$

$$D_i' = \frac{L_{yi}}{L_{xi}}\left(\frac{L_{yi}^2}{4L_{xi}^2} + \frac{3}{4}\right)\left(5c_{xi}^2 - 3c_{yi}^2 + 96\right) \tag{22}$$

and c_{xi} and c_{yi} are as defined in (13).

C. Verification of the Benefits of Anisotropic Discretization

The closed-form expressions derived in the previous sections appear to allow independent compensation of c_{xi} and c_{yi} through the use of the mesh dimensions L_{yi} and L_{xi}, respectively. Since it was shown in Section II-A that only c_{y2} would be affected by the magnitude of the PML variable parameter, a reduction in L_{x2} only should be sufficient to compensate. To test this hypothesis, the simulations of Section II-B are repeated; however, in this investigation, only the mesh dimension L_{x2} is reduced.

To achieve this anisotropic meshing, a geometry similar to the PML terminated parallel-plate waveguide of Section II-A is used; however, the thickness of the PML layer is multiplied by a nominal factor. The geometry is then discretized using the triangle [7] mesh generator and then the resulting mesh is post-processed, compressing the dimensions within the PML layer by the same nominal factor in the normal direction, resulting in an identical geometry to that used in Section II-A, but with an anisotropically compressed mesh.

Fig. 5 shows the effect of a one-dimensional (1-D) mesh compression on the parallel-plate waveguide problem using edge-basis functions to model the reflection of the TEM mode from a 2-cm-thick PML truncation and mesh compression ratios of one, two, four, and eight in the direction normal to the PML interface. Both the results of a practical finite-element simulation and the predicted results using (17) for anisotropic discretization are presented. Excellent agreement is observed.

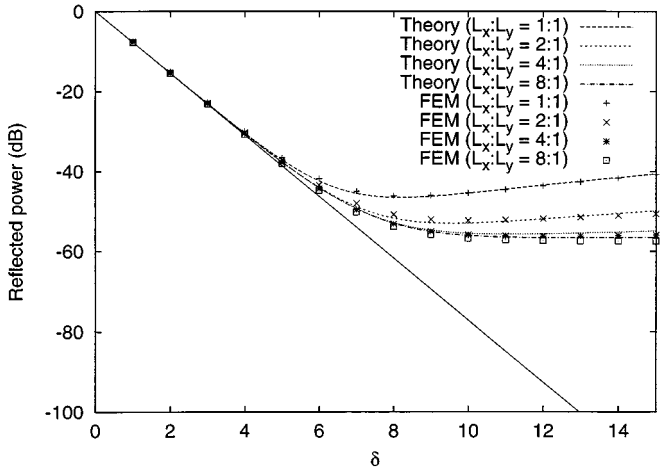

Fig. 6. Numerical reflection from a PML interface as a function of $\delta = \ln(1/R)$ with edge lengths of 2.0 mm and 1-D normal compression ratios of one, two, four, and eight in the PML region using an incident TM_1 mode at 8 GHz and node-basis functions. The lines indicate the reflection predicted by the closed-form expressions, while the points represent the reflection actually observed from a finite-element simulation using a practical mesh. The ideal reflection is also shown.

Examination of Fig. 5 shows that the 1-D compression is just as effective as the uniform reduction of edge length. The important advantage of 1-D compression is that since the mesh density increases in only a single dimension, only a linear increase in the number of unknowns results. Uniform mesh refinement would require a quadratic increase in the number of unknowns, as demonstrated in [3].

As discussed in [8], improved PML performance can be obtained through tapering the PML variable parameter with depth in the PML layer. It should also be desirable to vary the mesh compression along with the PML absorption to minimize the numerical reflections from a PML boundary. This hypothesis could form the basis of a separate investigation.

This technique could be applied to a 3-D simulation. In that situation, the mesh compression required should still only be 1-D and, hence, scale linearly, compared to the cubic increase required for uniform refinement.

Many practical problems involve a PML termination that surrounds the problem requiring the implementation of corner regions [9]. In this instance, 1-D compression of the PML regions would result in a uniform compression of the corners requiring additional unknowns. Even so, this approach should be far more efficient than an equivalent uniform compression of all of the PML regions.

Fig. 6 shows the result of applying the same procedure to the parallel-plate problem as excited with the TM_1 mode at 8 GHz and modeled using node elements. The predicted reflection is again in good agreement with the observed behavior from the FEM using a practical mesh, however, it is also evident that the limit of the gains offered by mesh compression have been reached and, thus, $8\times$ compression offers little advantage over a $4\times$ compression. This surprising result can be explained as follows.

Since the PML variable parameter (a_{pml}), as defined in (4), is inversely proportional to frequency, as the frequency increases, the magnitude of the PML parameter becomes rapidly smaller. At 8 GHz, a_{pml} is 80 times smaller than it is at 100 MHz. Now, since the reflection error at a PML interface has been shown in Section II-A to scale as the square of a_{pml}, the reflection error due to the PML is orders of magnitude smaller at 8 GHz than at 100 MHz. Further, since the frequency is higher and the base edge length has remained constant at 2 mm, the c values in the air-filled region have increased linearly with frequency and, thus, it is proposed that the numerical errors resulting from the discretization unrelated to the presence of the PML dominate once the mesh compression exceeds a factor of four. The only way to further reduce this error level would be to uniformly refine the mesh until the PML again becomes the dominant source of error.

It is worth noting that the effect of the mesh compression on the condition number of the finite-element number was briefly investigated. Details of this investigation can be found in [10], where it is noted that a thorough analysis of the effects of mesh compression on the finite-element condition number would itself form the basis of a separate study. To summarize, in most cases, the compressed simulation exhibited an equal or better condition number than the uncompressed case. Conceptually this make sense since the compression restores balance to the magnitudes of c_{xi} and c_{yi} and, hence, balances the various entries in the finite-element matrix.

IV. Conclusions

The closed-form expressions for numerical dispersion and reflection in finite-element simulations derived in [5] have been developed for specific application to the case of a PML boundary. The expressions derived provide excellent models of the behavior of a practical PML boundary for both edge and node elements for fundamental and higher order modes. As such, these expressions should be of great use in the design of absorbing boundaries of optimal effect requiring the minimum unknowns. In particular, it is suggested that they be used to examine the PML taper profiles for efficient and effective broad-band PML truncations.

Beyond this application, examination of the form of the relations suggested that mesh refinement in a single dimension only is required to reduce reflections at a PML boundary. To test this proposal, closed-form expressions for anisotropically dimensioned triangles were defined, and it was discovered that, indeed, only a 1-D compression was required. Practical simulations of PML truncations with anisotropically compressed meshes verified this hypothesis, demonstrating a new and economical means of implementing a highly effective PML truncation.

References

[1] J. P. Bérenger, "A perfectly matched layer for the absorption of electromagnetic waves," *J. Comput. Phys.*, vol. 114, no. 2, pp. 185–200, Oct. 1994.

[2] Z. S. Sacks, D. M. Kingsland, R. Lee, and J. F. Lee, "A perfectly matched anisotropic absorber for use as an absorbing boundary condition," *IEEE Trans. Antennas Propagat.*, vol. 43, pp. 1460–1462, Dec. 1995.

[3] A. C. Polycarpou, M. R. Lyons, and C. A. Balanis, "An optimized anisotropic PML for the analysis of microwave circuits," *IEEE Microwave Guided Wave Lett.*, vol. 8, pp. 30–32, Jan. 1998.

[4] J. Fang and Z. Wu, "Closed-form expression of numerical reflection coefficient at PML interfaces and optimization of PML properties," *IEEE Microwave Guided Wave Lett.*, vol. 6, pp. 332–334, Sept. 1996.
[5] A. Mitchell, D. M. Kokotoff, and M. W. Austin, "Closed-form expressions for the numerical dispersion and reflection in FEM simulations involving biaxial materials," *IEEE Trans. Antennas Propagat.*, vol. 49, pp. 158–164, Feb. 2001.
[6] A. Mitchell, T. Aberle, D. M. Kokotoff, and M. W. Austin, "An anisotropic PML for use with biaxial media," *IEEE Trans. Microwave Theory Tech.*, vol. 47, pp. 374–377, Mar. 1999.
[7] J. R. Shewchuk, "Triangle 1.3: A two-dimensional quality mesh generator and Delaunay triangulator," School Comput. Sci., Carnegie-Mellon Univ., Pittsburgh, PA, software, 1996.
[8] A. C. Polycarpou, M. R. Lyons, and C. A. Balanis, "A two dimensional finite element formulation of the perfectly matched layer," *IEEE Microwave Guided Wave Lett.*, vol. 6, pp. 338–340, Sept. 1996.
[9] S. G. Gedney, "An anistropic perfectly matched layer-absorbing medium for the truncation of FDTD lattices," *IEEE Trans. Antennas Propagat.*, vol. 44, no. 12, pp. 1630–1639, Dec. 1996.
[10] A. D. Mitchell, "Efficient PML boundaries for anisotropic waveguide simulations using the finite element method," Dept. Commun. Electron. Eng., Ph.D. dissertation, RMIT, Melbourne, Vic., Australia, 1999.

Arnan Mitchell (S'97–M'00) was born in Dublin, Ireland, on February 20, 1973. He received the B.Tech. degree in optoelectronics (with honors) from Macquarie University, N.S.W., Australia, in 1993, and the Ph.D. degree from the Royal Melbourne Institute of Technology (RMIT) University, Melbourne, Vic., Australia.

He is currently an Australian Photonics CRC Research Fellow with the Department of Communication and Electronic Engineering, RMIT University, where he investigates broad-band and specialized integrated optical modulators and RF photonic components for communications and signal-processing applications and maintains an active interest in the research of numerical methods required for the design of RF photonic integrated devices.

David M. Kokotoff (S'85–M'85) received the B.S.E.E. degree from Lafayette College, Easton, PA, in 1985, the M.S.E.C.E. degree from the University of Massachusetts at Amherst, in 1987, and the Ph.D. degree from Arizona State University, Tempe, in 1995.

From 1987 to 1992, he was with the Atlantic Aerospace Electronics Corporation, Greenbelt, MD, where he was a member of the Advanced Antenna Development Group. Upon completion of his doctoral degree, he joined the Department of Communication and Electronic Engineering, Royal Melbourne Institute of Technology (RMIT) University, Melbourne, Vic., Australia, where he was a Lecturer from 1996 to 1999. He is currently an Antenna Design Engineer with Gabriel Electronics, Scarborough, ME. His professional interests focus on applied electromagnetics, emphasizing the computer-aided design of antennas, microwaves, and optical devices.

Michael W. Austin (M'83) received the B.Eng. degree in communication engineering (with distinction) and Masters degree in electronic engineering from the Royal Melbourne Institute of Technology (RMIT) University, Melbourne, Vic., Australia, in 1977 and 1980, respectively, and the Ph.D. degree in electronic engineering from the University of London, London, U.K., in 1982.

From 1979 to 1982, he was a Research Fellow with British Telecom Research Laboratories, Ipswich, U.K., where he was involved with the field of integrated optics in III–V semiconductors. Since 1982, he has been a member of the academic staff of the Department of Communication and Electronic Engineering, RMIT University (recently renamed the School of Electrical and Computer Systems Engineering). He is currently a Professor and has been Director of RMIT's Microelectronics and Materials Technology Center (MMTC) since 1994. In 1988, he spent six months as an Invited Researcher at the Communications Research Laboratory, Tokyo, Japan, where he was involved with an L-band phased-array antenna for aeronautical mobile satellite communications. His research interests include the theoretical and experimental study of guided-wave optical devices. He is particularly interested in the fabrication of wide-band optical intensity modulators in lithium niobate.

Prof. Austin is a Fellow of the Institution of Engineers, Australia. He is a senior member of the Information, Telecommunications, and Electronics Engineering (ITEE) Society.